



# 1 **Relevance of near-surface soil moisture vs. terrestrial water storage** 2 **for global vegetation functioning**

3 Prajwal Khanal<sup>1,2</sup>, Anne J. Hoek Van Dijke<sup>1</sup>, Timo Schaffhauser<sup>2</sup>, Wantong Li<sup>1</sup>, Sinikka J. Paulus<sup>1,3</sup>,  
4 Chunhui Zhan<sup>1,4</sup>, René Orth<sup>1</sup>

5 <sup>1</sup>Department of Biogeochemical Integration, Max Planck Institute for Biogeochemistry, Hans-Knöll-Straße 10, 07745 Jena, -  
6 Germany

7 <sup>2</sup>Chair of Hydrology and River Basin Management, Technical University of Munich, Arcisstraße 21, 80333 Munich, Germany

8 <sup>3</sup>Chair of Terrestrial Ecohydrology, University of Jena, Burgweg 11, 07749, Jena, Germany

9 <sup>4</sup>Land Surface-Atmosphere Interactions, Technical University of Munich, TUM School of Life Sciences Weihenstephan,  
10 85354 Freising, Germany

11 *Correspondence to:* Prajwal Khanal (ktm.prajwalkhanal@gmail.com)

12 **Abstract.** Soil water availability is an essential prerequisite for vegetation functioning. Vegetation takes up water from varying  
13 soil depths depending on the characteristics of their rooting system and soil moisture availability across depth. The depth of  
14 vegetation water uptake is largely unknown across large spatial scales as a consequence of sparse ground measurements. At  
15 the same time, emerging satellite-derived observations of vegetation functioning, surface soil moisture and terrestrial water  
16 storage, present an opportunity to assess the depth of vegetation water uptake globally. In this study, we characterise vegetation  
17 functioning through the Near-Infrared Reflectance of Vegetation (NIRv), and compare its relation to (i) near-surface soil  
18 moisture from ESA-CCI and (ii) total water storage from GRACE at the monthly time scale during the growing season. The  
19 relationships are quantified through partial correlations to mitigate the influence of confounding factors such as energy-related  
20 variables. We find that vegetation functioning is generally more strongly related to near-surface soil moisture, particularly in  
21 semi-arid regions and areas with low tree cover. In contrast, in regions with high tree cover and in arid regions, the correlation  
22 with terrestrial water storage is comparable to or even higher than with near-surface soil moisture, indicating that trees can and  
23 do make use of their deeper rooting systems to access deeper soil moisture, similar to vegetation in arid regions. In line with  
24 this, an attribution analysis that examines the relative importance of these soil water storages for vegetation reveals that they  
25 are controlled by (i) water availability influenced by the climate and (ii) vegetation type reflecting adaptation of ecosystems  
26 to local water resources. Next to variations in space, the vegetation water uptake depth also varies in time. During dry periods,  
27 the relative importance of terrestrial water storage increases, highlighting the relevance of deeper water resources during rain-  
28 scarce periods. Overall, the synergistic exploitation of state-of-the-art satellite data products to disentangle the relevance of  
29 near-surface vs. terrestrial water storage for vegetation functioning can inform the representation of vegetation-water  
30 interactions in land surface models to support more accurate climate change projections.



## 31 **1. Introduction**

32 The regulation of water, energy, and biogeochemical cycling between land and atmosphere is primarily dependent on  
33 vegetation. In addition, global vegetation provides essential ecosystem services such as food production and uptake of some  
34 of the anthropogenic carbon dioxide emissions (Keenan & Williams, 2018). Vegetation growth depends on nutrient, water and  
35 energy availability. As a result, on a global scale, there are regions with energy or water limited vegetation functioning (Orth,  
36 2021). In energy-limited regions, the functioning of vegetation is controlled by radiation and temperature, as they often lack  
37 sunny and warm conditions but have ample soil moisture. In contrast, soil moisture becomes critical for vegetation growth in  
38 water-limited regions. Plant photosynthesis involves opening the stomata for the uptake of CO<sub>2</sub>, while at the same time water  
39 is lost through transpiration. However, in water-limited conditions, plants can reduce the stomatal opening to avoid water loss,  
40 leading to a decrease in photosynthesis. Hence, variations in soil moisture are likely to affect vegetation functioning in water-  
41 limited conditions. Moreover, climate change has led to an expanded water limitation on vegetation (Denissen et al., 2022)  
42 and increased vegetation sensitivity to soil moisture (Li et al., 2022). For these reasons, it is essential to better understand the  
43 dependence of vegetation functioning on soil moisture to comprehend their coping mechanisms during drought to predict the  
44 future of global water, energy, and carbon cycles.

45  
46 Plants extract water from varying soil depths based on the positioning of their roots and the availability of soil moisture. In  
47 general, the plant water uptake depth further differs spatially across different climate regimes and vegetation types, and  
48 temporally between seasons. Vegetation in arid regions is more susceptible to fluctuations in near-surface soil moisture  
49 compared to vegetation in humid regions (Xie et al., 2019). Grasses, which generally have shorter roots than trees and shrubs,  
50 are more reliant on near-surface moisture than deeper moisture (Schenk & Jackson, 2002). Further, root water uptake profiles  
51 vary within individual plant types according to above-ground biomass and age, with larger and older trees having deeper roots  
52 capable of extracting water from deeper soil layers (Schenk & Jackson, 2002; Tao et al., 2021). Additionally, within similar  
53 climate regimes, plant water uptake varies across topographic positions. Upland and lowland roots tend to be shallower, making  
54 vegetation more reliant on near-surface soil moisture, while roots go deeper in steep terrain between these landscapes to access  
55 both surface and deep moisture (Fan et al., 2017).

56  
57 Though spatial variations of plant water uptake depths across vegetation types and climate regimes, and temporal shift during  
58 dry-months, are widely studied at point scale, inadequate deep soil moisture records pose a major obstacle to study vegetation  
59 root water uptake at a global scale. Microwave remote sensing allows to infer near-surface soil moisture dynamics globally.  
60 However, such data may not fully represent root-zone soil moisture as microwaves can only propagate through the top few  
61 centimetres in soil (Capehart & Carlson, 1997). Land surface models provide an alternative source of global soil moisture data  
62 across depths, but they are subject to uncertainties arising from meteorological data, inaccurate knowledge of soil and  
63 vegetation characteristics, and the representation of complex processes such as photosynthesis, infiltration, and evaporation



64 (Koster et al., 2009; Seneviratne et al., 2010). Hence, some studies have employed reanalysis-based soil moisture estimates,  
65 to investigate the relationship between vegetation and soil moisture at the global (Li et al., 2021; Miguez-Macho & Fan, 2021);  
66 but those are likely to be impacted by model assumptions affecting soil moisture dynamics, particularly for deeper layers where  
67 less observational constraints are available. Thus, studying vegetation interactions with the entire water column, including  
68 near-surface and deep soil moisture, at a global scale using exclusively observation-based dataset is imperative to enhance the  
69 understanding of relevance of near-surface and deep soil moisture for vegetation functioning.

70

71 The Gravity Recovery and Climate Experiment (GRACE) satellite mission, launched in 2002, provides total water storage  
72 (TWS) anomalies observations at the global scale and offers a unique opportunity to investigate the relationship between  
73 vegetation and the total water column. Furthermore, the inter-annual carbon dioxide growth rate in the atmosphere has been  
74 found to be well correlated with the total water storage anomalies on a global scale, underlining the relevance of total water  
75 column for vegetation functioning (Humphrey et al., 2018). The TWS captures not only soil water but also snow and ice,  
76 canopy water, surface water, and groundwater. TWS anomalies can be used to estimate the variation of overall water  
77 availability (near-surface + deep soil moisture) for vegetation under (i) snow-free conditions, and assuming that (ii) water  
78 storage variations in lakes or groundwater are negligible at the monthly time scale, (iii) and canopy water storage is much  
79 smaller than soil water storage and hence also negligible.

80

81 This study focuses on understanding the relevance of near-surface vs. total water storage for vegetation functioning on a global  
82 scale using observation-based datasets, thereby inferring vegetation's large-scale water uptake depth from observation-based  
83 datasets. For this purpose, we utilise TWS and near-surface soil moisture and correlate them with vegetation functioning,  
84 represented by Near-Infrared Reflectance of Vegetation (NIR<sub>v</sub>). In particular, we analyse (1) what is the relevance of near-  
85 surface soil moisture vs. the terrestrial water storage for vegetation functioning?, (2) how does the importance of near-surface  
86 soil moisture vs. terrestrial water storage change during dry months? and (3) how do climatic, vegetation, and topographic  
87 characteristics explain the variability in the relevance of near-surface vs. terrestrial water storage for vegetation functioning?

## 88 2. Data and Methodology

89 **Table 1: Table summarising all the datasets.**

Datasets	Variables	Source	Spatial Resolution	References
Vegetation Functioning	Near Infrared Reflectance of Vegetation (NIR <sub>v</sub> )	MODIS/MOD13C1 v061	0.05 degree	(Badgley et al., 2017)
	Solar Induced Chlorophyll Fluorescence (SIF)	GOME-2	0.5 degree	(Köhler et al., 2015)



<b>Soil Water Storage</b>	Near-surface soil moisture (SSM)	ESA-CCI v04.4	0.25 degree	(Dorigo et al., 2017)
	Total Water Storage (TWS) Anomalies	GRACE	0.5 degree	(Landerer & Swenson, 2012)
<b>Meteorological</b>	Air Temperature ( $T_a$ )	ERA-5	0.25 degree	(Hersbach et al., 2020)
	Precipitation (P)			
	Net Radiation ( $R_n$ )			
<b>Vegetation and Land cover class</b>	Tree cover fraction	VFC5KYR	0.05 degree	(Hansen, Matthew & Song, Xiao-Peng, 2018)
	Land cover data	ESA-CCI	0.05 degree	ESA. Land Cover CCI Product User Guide Version 2. Tech. Rep. (2017)
<b>Topographical data</b>	Elevation	Earthenv	1 km	(Amatulli et al., 2018)
	Slope			
<b>Soil data</b>	Fraction of sand	FAO	0.05 degree	(Reynolds et al., 2000)
	Fraction of clay			
<b>Irrigation</b>	Percentage of Irrigated area	HID	5 arcmin	(Siebert et al., 2015)

90

## 91 **2.1 Data**

### 92 **2.1.1 Vegetation Functioning:**

93 In our study, vegetation functioning is characterised by satellite measurements of Near-Infrared Reflectance of vegetation  
 94 (NIRv) and Solar Induced Fluorescence (SIF) (**Table 1**). NIRv is the product of near-infrared reflectance and the normalised  
 95 difference vegetation index (NDVI) and represents the vegetation structure and vegetation greenness (Badgley et al., 2017).  
 96 The NIRv data is available at a high spatial resolution of 0.05°, and the original 16-day data was aggregated to the monthly  
 97 NIRv data. SIF is directly related to the photosynthetic activity of plants because the excess energy from sunlight, that triggers  
 98 the light reaction during photosynthesis, is dissipated by leaf as chlorophyll fluorescence (Mohammed et al., 2019). SIF data  
 99 is derived from the Global Ozone Monitoring Experiment (GOME-2), because GOME-2 provides relatively reliable data over  
 100 a long period (2007-2018). The 0.5° spatial and 16-day temporal resolution SIF data is processed into monthly data as described  
 101 by (Köhler et al., 2015).

102

103 The high spatial resolution of NIRv allows for a detailed study of the correlation of vegetation functioning with soil water  
 104 availability. Therefore, we performed the main analyses using NIRv data. However, SIF is more sensitive to drought stress  
 105 than NIRv (Qiu et al., 2022). Therefore, we perform additional analyses with SIF to show that the relationships hold for a  
 106 different and more direct indicator of vegetation functioning.



### 107 **2.1.2 Soil Water Storage**

108 This study includes two different measures of soil water availability. The near-surface soil moisture (SSM) provides an  
109 estimate of water availability in the top layer of the soil, while the Terrestrial Water Storage (TWS) Anomaly provides an  
110 estimate of the overall water column of the soil. The SSM data is derived from the European Space Agency (ESA) Climate  
111 Change Initiative Program (CCI), which combines active and passive satellite microwave measurements to provide reliable  
112 estimates of SSM (Dorigo et al., 2017). The ESA CCI soil moisture data, at a daily temporal resolution, was aggregated to  
113 monthly temporal resolution. The TWS Anomaly data is derived from the GRACE mission, which measures changes in the  
114 Earth's gravity field (Landerer & Swenson, 2012). Here, we use the JPL-Mascons product of TWS Anomalies which is  
115 available at a 0.5° spatial and monthly temporal resolution.

### 116 **2.1.3 Meteorological Data**

117 Employed climate variables include monthly air temperature ( $T_a$ ), precipitation (P), and net radiation ( $R_n$ ) from the ERA5  
118 reanalysis products at a 0.25° spatial resolution. The aridity index is calculated from the ratio between the long-term mean  $R_n$   
119 ( $\text{mm y}^{-1}$ ) ( $1 \text{ MJ/sq.m/day} = 0.408 \text{ mm/day}$ ) and P ( $\text{mm y}^{-1}$ ) for each grid cell (Budyko, 1974). In addition, the mean and  
120 standard deviation of the climate variables are calculated and incorporated in the attribution analysis (**Section 2.2.3**).

### 121 **2.1.4 Vegetation, soil, and topography data**

122 To evaluate the resulting correlation of vegetation functioning and water storages with respect to vegetation characteristics,  
123 we employ the tree cover fraction data from the AVHRR vegetation continuous fields products (VCF5KYR,  
124 <https://lpdaac.usgs.gov/products/vcf5kyrv001/>) (Hansen, Matthew & Song, Xiao-Peng, 2018). For this purpose, the mean of  
125 tree cover fraction for the years between 2007 and 2016 is calculated.

126  
127 Topographical variables such as elevation and slope are incorporated along with other climatological variables to determine  
128 the relative contribution of different variables to the correlation between vegetation functioning and water storage. Topographic  
129 data at a 5 km resolution were downloaded from the EarthEnv. These data are calculated based on the 250 m GMTED dataset,  
130 and compared against the 90 m SRTM 4.1 dev dataset. The data were resampled to a coarser resolution of 5 km using various  
131 aggregation techniques, details of which are in (Amatulli et al., 2018). Furthermore for each grid cell, the fraction of sand and  
132 clay in soil (Reynolds et al., 2000) along with the percentage of irrigated area (Siebert et al., 2015) were considered in  
133 attribution analysis.

134



## 135 2.2 Methodology

### 136 2.2.1 Data pre-processing

137 A flowchart of the data pre-processing and analyses is presented in **Figure S1**. The time period of analysis is from 2007 to  
138 2018 constrained by the concurrent availability of all involved datasets. All the analyses were performed in monthly temporal  
139 resolution and at  $0.05^\circ$  spatial resolution (for NIRv) and  $0.5^\circ$  spatial resolution (for SIF). The SSM and TWS data were initially  
140 available at  $0.25^\circ$  and  $0.5^\circ$  resolution, but were disaggregated or aggregated to  $0.05^\circ$  or  $0.5^\circ$  degrees, depending on the spatial  
141 resolution of the analysis performed, based on the assumption that the soil water storage anomalies are representative over  
142 larger areas. Also the meteorological data and vegetation, soil, and topographic data were resampled into the same resolution.  
143 After aggregating all the datasets to  $0.05^\circ$  resolution, the monthly anomalies were calculated by subtracting the long term mean  
144 monthly cycle and by removing linear trends. A SIF threshold was applied in each grid cell to filter out non-growing season  
145 data. For this purpose, we filtered out all the months from 2007-2018 when the mean-monthly SIF value was below the  
146 threshold of  $0.2 \text{ mW/m}^2/\text{sr/nm}$ . We apply an additional temperature threshold ( $T_a > 5^\circ\text{C}$ ) to remove the months with frozen  
147 soil and snow cover, similar to (Li et al., 2021). Last, all months with missing soil water storage or vegetation functioning  
148 records were excluded.

### 149 2.2.2 Calculate the relevance of near-surface (SSM) soil moisture and terrestrial water storage (TWS) for vegetation 150 functioning

151 We calculated the spearman correlation between vegetation functioning (NIRv) and soil water storages (SSM and TWS) for  
152 each grid cell during growing season months when observations for at least 40 months were available. In addition to soil  
153 moisture, also air temperature ( $T_a$ ) and net radiation ( $R_n$ ) affect the vegetation functioning. To focus exclusively on the effects  
154 of water availability on vegetation functioning, we corrected for the confounding effects of  $T_a$  and  $R_n$ , by computing the partial  
155 correlation between NIRv and water storages while controlling for  $T_a$  and  $R_n$ . Since we focus on understanding the role of soil  
156 moisture on vegetation functioning, which is primarily critical in water-limited conditions, we removed the grids cells with  
157 insignificant ( $p < 0.05$ ) and negative partial correlations from our analysis. Such negative partial correlations may hint at  
158 vegetation's converse effect on soil moisture (when increasing vegetation activity depletes the soil moisture) and a negative  
159 correlation could occur in the grid cells where water limits vegetation productivity through oxygen limitation (Ohta et al.,  
160 2014).

161  
162 To analyse how the importance of SSM and TWS changes during dry months, we selected the months with the lowest 10%  
163 SSM for each grid cell. The partial correlations between NIRv and water storages,  $r(\text{NIRv} \sim \text{SSM})$  and  $r(\text{NIRv} \sim \text{TWS})$  were  
164 calculated separately for dry months. To focus on vegetation response to similar extent of dryness spatially, only grid cells  
165 with greater than 100 monthly observations were considered for the dry months analysis. In addition, only the grid cells which  
166 had significant partial correlation in growing season months were included for the dry months analysis.



167

168 After computing the partial correlations, we grouped the grid cells by aridity and tree cover or land cover classes and calculated  
169 the mean correlation, for each aridity-tree cover class with sufficient number of observations for both growing season and dry  
170 months. This allowed us to analyse the evolution of correlations and the difference between the partial correlation across aridity  
171 and vegetation classes.

172

173 Moreover, to test the robustness of the results, we did additional correlation analyses, for which we correlated the SIF (instead  
174 of NIRv) with SSM and TWS. The analyses with SIF were performed at a spatial resolution of  $0.5^\circ$ , at which SIF data was  
175 available.

### 176 **2.2.3 Attribution Analysis**

177 We used a random forest model to understand the spatial variability in the relevance of SSM versus TWS for NIRv. Random  
178 forest is a nonparametric based regression algorithm which does not require any statistical assumptions on the predictor and  
179 target variables which makes it particularly useful for detecting the nonlinear relationship (Breiman, 2001). Given potential  
180 nonlinear impacts of various factors (climate, soil types, vegetation) on the relationship between moisture storages and  
181 vegetation functioning, this study employed the random forest method to assess the relative contributions of these variables.

182

183 In our study, 13 predictors were included in the random forest model based on their potential physical relevance to the target  
184 variable, which is the difference in correlation between SSM and TWS with NIRv in growing season months. These predictors  
185 included mean and standard deviation of climate variables ( $T_a$ ,  $R_n$ , and P), aridity index, topographical variables (elevation and  
186 slope), vegetation variable (tree cover), soil-related variables (fraction of clay and sand), and percentage of irrigated areas for  
187 each grid cell. We calculated the mean and standard deviation of the climate variables only during the growing months (the  
188 months with  $SIF_{\text{mean-monthly}} < 0.2 \text{ mW/m}^2/\text{sr/nm}$  were excluded). Furthermore, only the grid cells having significant and positive  
189 partial correlation between NIRv and SSM as well as NIRv and TWS during growing season-months were included in the  
190 random forest analysis. For training a random forest model, we used the “xgboost” package in R (Chen & Guestrin, 2016).

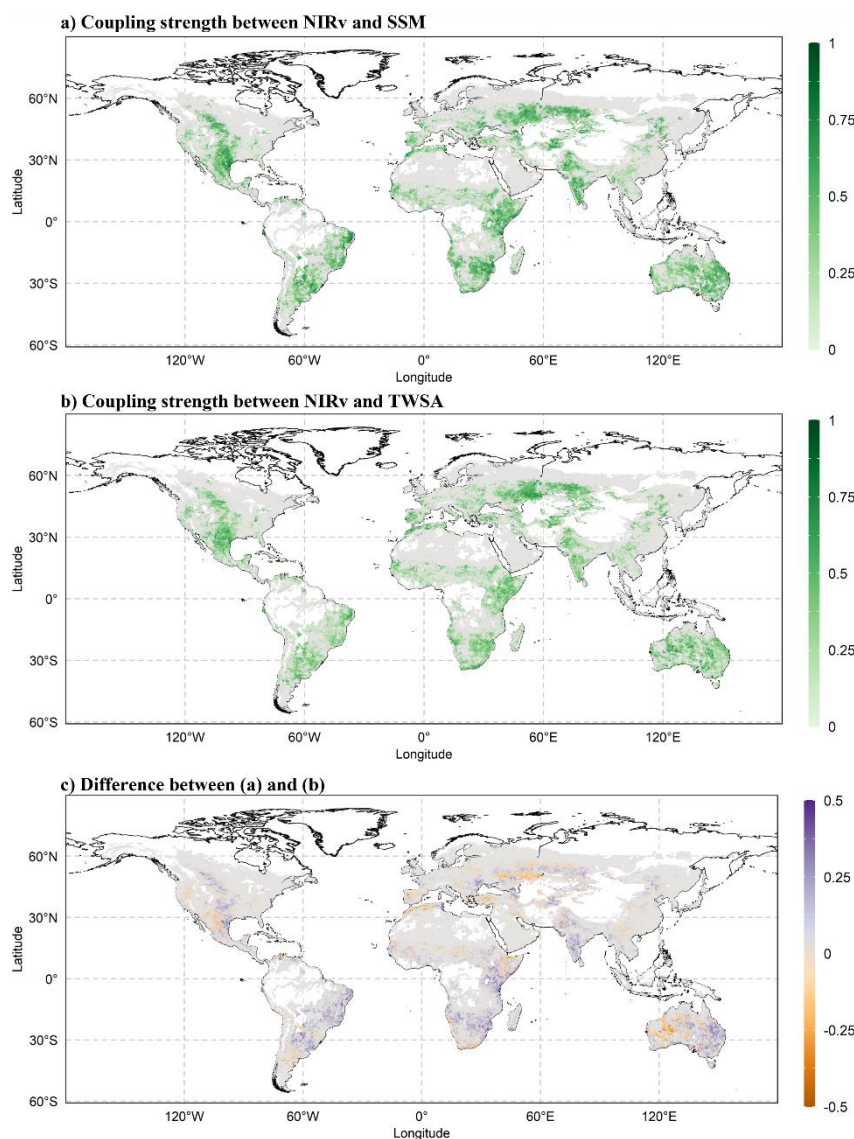
191

192 We further incorporate SHAP (SHapley Additive exPlanations) values for interpreting the predictions of the random forest  
193 model (Lundberg et al., 2020). The SHAP value for a feature is the average difference in prediction of the model when that  
194 feature is included compared to when it is excluded, over all possible combinations of features. By calculating SHAP values  
195 for each feature in the model, we identified which features were most important in explaining the spatial variability in the  
196 relevance of SSM versus TWS. For calculating the SHAP values, we employed “SHAPforxgboost” package in R.



197 **3. Results and Discussion**

198 **3.1 Coupling of vegetation functioning with surface soil moisture and total water storage in the growing season**



199

200 **Figure 1: Coupling strength between vegetation functioning (NIRv) and (a) near-surface soil moisture (SSM), and (b) total water**  
201 **storage (TWS) during the growing season months. Monthly anomalies of all variables are used to calculate the partial correlation.**  
202 **(c) Difference between (a) and (b). The purple colour in (c) indicates the greater partial correlation of NIRv with SSM compared to**  
203 **the partial correlation of NIRv with TWS while orange colour indicates the opposite. Grid cells with significant ( $p < 0.05$ ) and**  
204 **positive relationships for both correlations (a) and (b) are shown in (c) with blueish and orange colours. Light grey colour indicates**  
205 **insignificant and/or negative partial correlations between NIRv and water storage.**

206 The partial correlation of NIRv with near-surface soil moisture varies globally during growing-season months (**Figure 1a**).

207 NIRv demonstrates stronger correlation with near-surface soil moisture within semi-arid climates, Central North America,



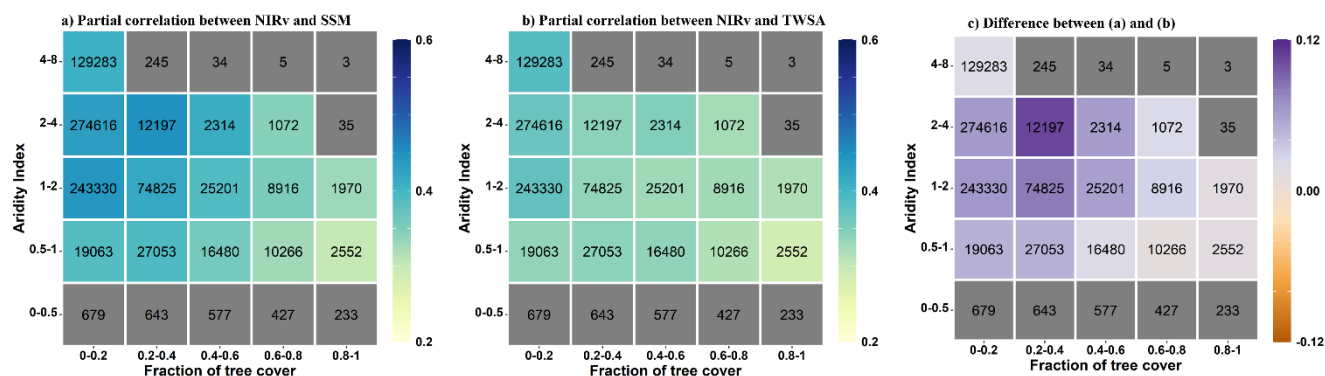


208 South America, regions in South Africa and Australia. The correlation is stronger in Southern Europe and the Mediterranean  
 209 region compared to central and Northern Europe. The correlation gradient from the hot and dry Mediterranean region to wet  
 210 and cold Northern Europe corresponds to the gradient of water-limited ecosystems to energy-limited ecosystems obtained in  
 211 other studies (Denissen et al., 2022; Teuling et al., 2009).

212  
 213 The global correlation of NIRv with TWS follows a similar pattern as with SSM (**Figure 1b**) in growing-season months. The  
 214 correlation of NIRv with TWS is higher in drier central northern America and Australia compared to other regions. The  
 215 similarities in the correlation of NIRv with SSM and TWS are expected because the monthly anomalies of SSM and TWS are  
 216 highly correlated during growing season months in most of our study area (**Figure S2**).

217  
 218 The difference between the partial correlation of NIRv with SSM and TWS (**Figure 1c**) indicates that the NIRv correlates  
 219 stronger with TWS in Western America, Southern Europe, and arid regions of Australia compared to other regions globally  
 220 during growing-season months. In South America and Southern Africa, however, the NIRv shows a stronger correlation with  
 221 SSM. It is difficult to determine which soil water storage (SSM or TWS) is more critical for vegetation, because the near-  
 222 surface soil moisture is included in the measurements of TWS, and both datasets have very different noise levels.

223



224

225 **Figure 2: Summarising the coupling strengths of vegetation functioning (NIRv) with (a) near-surface soil moisture (SSM) and (b)**  
 226 **terrestrial water storage (TWS) in the growing season-months across climate (aridity index) and vegetation regimes (fraction of tree**  
 227 **cover). (c) shows the difference between (a) and (b). Numbers within the boxes denote the number of grid cells for each aridity-tree**  
 228 **cover class. Aridity-tree cover classes containing less than 1000 grid cells are shown in grey. The colour bar indicates a mean partial**  
 229 **correlation for each class. Only grid cells with significant ( $p < 0.05$ ) and positive relationships are considered.**

230

231 Next, we analyse the partial correlation between NIRv and soil water storages across different aridity and tree cover fraction  
 232 classes during growing season months. For this, we group the grid cells into different aridity and tree cover fraction classes  
 233 and then compute mean partial correlation for each class with more than 1000 grid cells. We find that the partial correlation of  
 234 NIRv with SSM (**Figure 2a**) increases with increasing aridity for aridity index 0.5 – 4. This can be attributed to the



235 intensification of water stress on vegetation under increasingly arid conditions, resulting in a stronger correlation between  
236 NIRv and SSM. However, for a further increase in aridity (4-8), the strength of the correlation of NIRv with SSM declines.  
237 This is due to a low soil moisture availability and low temporal variability under extremely arid conditions (**Figure S7**). The  
238 pattern of increasing correlation along aridity index is also observed in the partial correlation between NIRv and TWS. (**Figure**  
239 **2b**).

240  
241 Furthermore, the correlation of NIRv with SSM decreases for higher tree cover fractions (**Figure 2a**). However, such a gradient  
242 along tree cover fraction is less pronounced in the partial correlation of the NIRv with TWS (**Figure 2b**). This overall depicts  
243 that the coupling of vegetation functioning with SSM is generally higher for non-forested areas compared to forested areas  
244 while this gradient is less pronounced in the case of TWS.

245  
246 It is difficult to conclude which soil moisture storage (SSM or TWS) is more important for a certain aridity-vegetation class  
247 because it inherently includes the difference in noise levels associated with SSM and TWS. However, we can compare the  
248 evolution of the gradient along tree cover or aridity index and assert how the relevance of SSM and TWS changes with varying  
249 tree cover or aridity index. Taking this into account, we find that NIRv correlates more strongly with near-surface soil moisture  
250 compared to terrestrial water storage in semi-arid regions with low tree cover (**Figure 2c**), suggesting that the vegetation  
251 preferentially takes up water from SSM whenever available to meet its transpiration demand. This might be due to lower  
252 energy expenditure on root water uptake, abundant nutrients and reduced chance of root water logging in the near-surface soil  
253 moisture (Andrew Feldman et al., 2022; Schenk & Jackson, 2002; Tao et al., 2021). Conversely, the correlation between the  
254 NIRv and TWS in arid areas (AI 4-8) and regions with a high fraction of tree cover is equivalent to or greater than that of  
255 SSM, suggesting that trees can utilise their extensive root systems to access deeper soil moisture, as observed in arid vegetation.  
256 This is consistent with previous studies reporting that the vegetation dependence on sub-surface soil moisture is higher in arid  
257 and seasonal-arid climates (Miguez-Macho & Fan, 2021).

258  
259 Note that while our analysis focuses on regions with water-controlled vegetation as denoted by significantly positive  
260 correlations between NIRv and the considered soil water storages, some of these grid cells are located in comparatively wet  
261 climate regimes with aridity index values between 0.5 and 1 (**Figure 2**). This highlights the relevance of non-climatic factors  
262 such as soil and vegetation types or topography in determining vegetation-water relationships in addition to the climate regime.  
263 Next to this, in **Figure 2c** it seems that the relevance of terrestrial water storage is comparatively higher in wet climate (aridity  
264 0.5-1) than in transitional climate regimes (aridity 1-2) as shown with the smaller correlation differences. This, however, is  
265 probably not the case and simply a reflection of reduced variability in surface soil moisture (**Figure S7**).

266  
267 To ascertain that our results are not impacted by outliers, we analysed the heatmaps with 10<sup>th</sup> and 90<sup>th</sup> percentile correlation  
268 values for each aridity-vegetation class, instead of the mean correlation value (**Figure S3**). This shows consistent patterns of

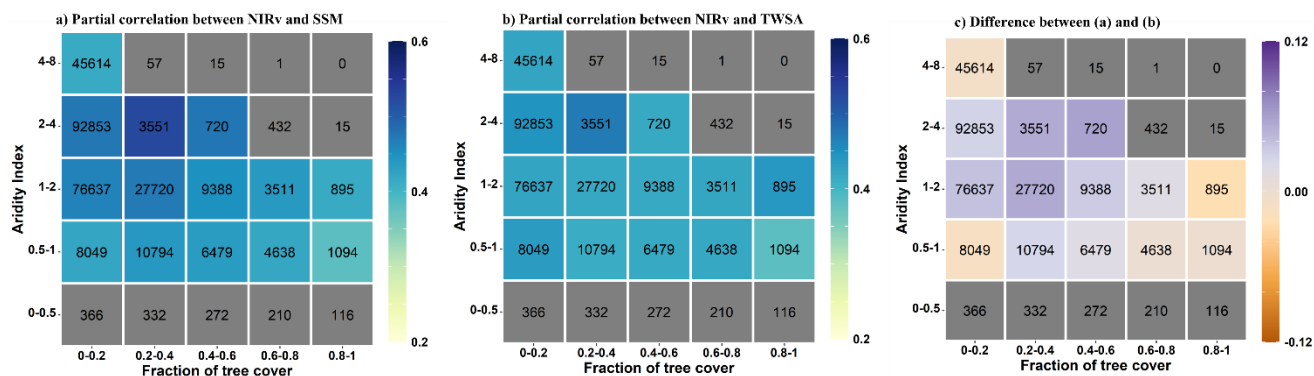


269 the partial correlation of NIRv with soil water storages as in **Figure 2** and indicates that the gradients with tree cover and  
 270 aridity are valid throughout the entire dataset.

271 **3.2 Coupling of vegetation functioning with surface soil moisture and total water storage in dry months**

272 The correlation between NIRv and soil water storage increases during dry months (**Figure 3a,b**) compared to growing season  
 273 months (**Figure 2a,b**). This increase is consistent for both SSM and TWS and across all tree cover fractions and aridity classes.  
 274 This is because the water limitation on vegetation increases in dry months and so does the vegetation’s sensitivity to the  
 275 moisture. During the dry months, the correlation with near-surface soil moisture tends to rise, but the correlation with terrestrial  
 276 water storage increases even more significantly (**Figure 3c**). This hints the relevance of deeper water resources during periods  
 277 of scarce rainfall. The partial correlation maps (**Figure S4**) also reveal that NIRv’s correlation with TWS increases more than  
 278 its correlation with SSM for most grid cells.

279



280

281 **Figure 3: Similar to Figure 2, but only considering the 10% driest months in each grid cell.**

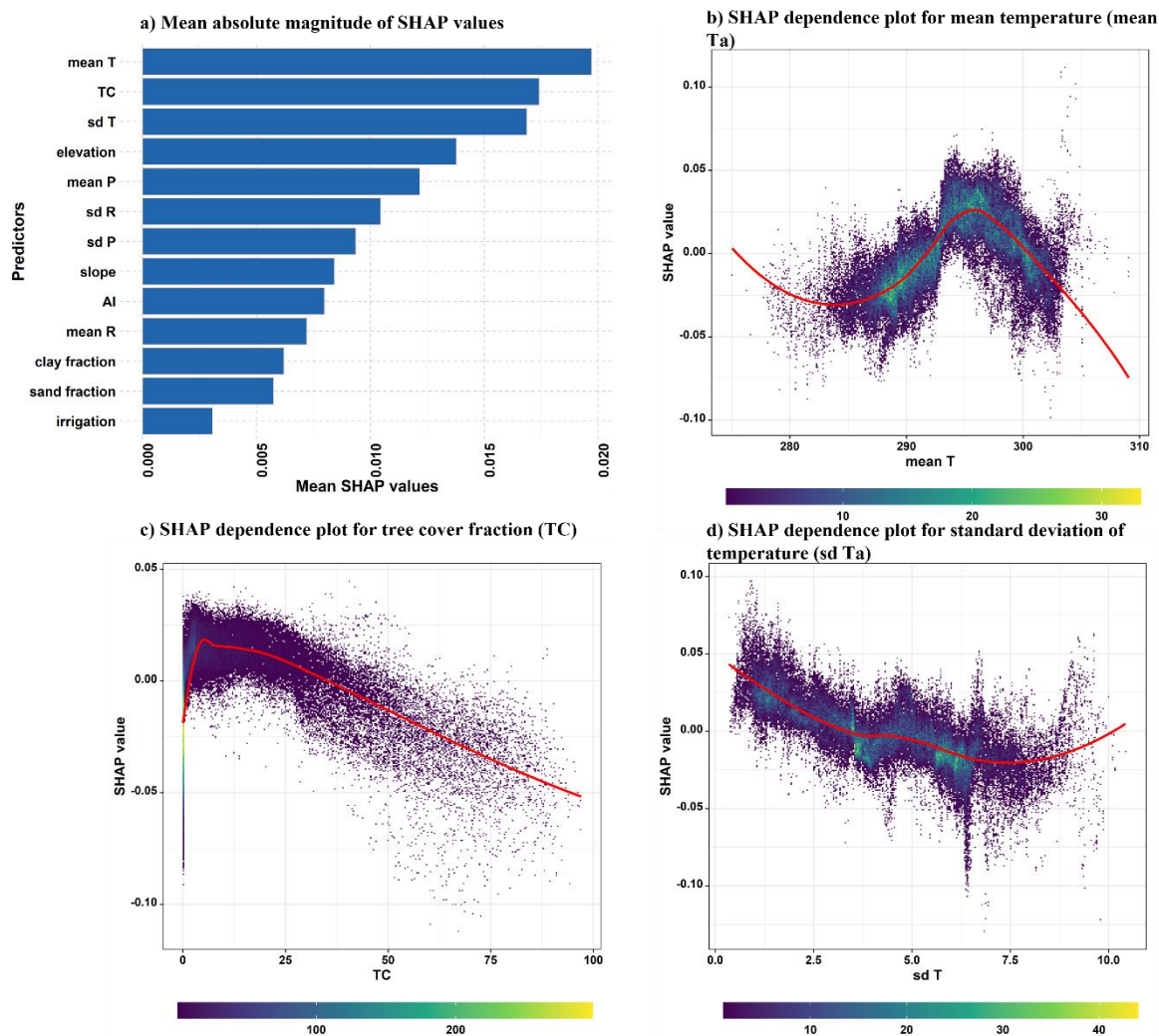
282 During dry months, the number of analysed grid cells (**Figure 3**) is lower compared to all growing season months (**Figure 2**).  
 283 We performed a reanalysis of the correlation patterns within aridity-tree cover classes by selecting only those grid cells that  
 284 displayed significant and positive partial correlation between NIRv and soil water storages during both the dry months and the  
 285 growing season months. The results demonstrate that the previously observed patterns remain valid, thereby eliminating the  
 286 impact of the differing numbers of grid cells analysed. (**Figure S5**).

287



288  
289

### 3.3 Climate, vegetation, and topographic controls on the relevance of surface soil moisture vs. total water storage on vegetation



290

291 **Figure 4:** (a) Global feature importance based on the mean absolute magnitude of the SHAP values. The higher the mean SHAP  
 292 values, the greater the predictor’s relevance. (b-d) Evaluation of SHAP values (=contributions to the correlation difference  
 293 illustrated in Figure 1c) against predictor values for the 3 most relevant predictors mean temperature during the growing season  
 294 months (mean  $T_a$ ), tree cover fraction (TC), and variability of temperature during the growing season months (sd  $T_a$ ). The colour  
 295 indicates the density of data points. For plotting (b), (c) and (d), only 10 percent random samples of the whole dataset are utilised.

296

297 We use a random forest model to understand the spatial variability in the relevance of SSM versus TWS for NIRv. The model  
 298 was trained with 13 climatic, vegetation, and topographic predictors against the target variable which is the difference of the  
 299 partial correlations of NIRv with SSM and TWS during growing season-months ( $R^2 = 0.64$ , see **methods section 2.2.3**). The  
 300 mean absolute SHAP value plot shows that the climate variables (mean and standard deviation of  $T_a$ ) and tree cover are most  
 important variables for explaining the spatial variability in the relative importance of SSM vs. TWS for vegetation functioning



301 **(Figure 4a)**. This overall highlights that the relative importance of SSM vs. TWS for the vegetation is broadly controlled by  
302 climate, influencing water availability and vegetation type, reflecting the local adaptation of ecosystem (Stocker et al., 2023).

303 The relative importance of SSM and TWS varies non-linearly with the mean growing season temperature **(Figure 4b)**. TWS  
304 tends to be more crucial for vegetation functioning in areas with low (approximately below 20°C) or high (above 27°C)  
305 growing season temperatures, while SSM has greater importance in regions with moderate growing season air temperatures.  
306 One possible explanation for this trend is that high temperatures induce a strong atmospheric water demand that dries near-  
307 surface soil layers, which leads vegetation to increase water extraction from deep soils. In contrast, SSM is more available  
308 during growing seasons characterised by moderate temperatures. Regions that experience relatively cold growing season  
309 temperatures exhibit stronger temperature and weather variability that may contribute to longer dry periods and, thus,  
310 emphasises the importance of deeper soil moisture for vegetation functioning. However, it should be noted that our findings  
311 regarding the relevance of TWS at high temperatures must be interpreted with caution due to the exclusion of most tropical  
312 forest regions from our analysis **(Figure S6)**. As a result, most warm regions are dry, and there are only a few hot and wet  
313 regions included in our training data.

314  
315 In addition to mean growing season  $T_a$ , tree cover fraction is an important factor in determining the relevance of SSM and  
316 TWS for vegetation functioning **(Figure 4c)**. Regions with a high tree cover are more dependent on TWS, as trees generally  
317 have deeper root systems that allow them to adjust water uptake between different depths (Tao et al., 2021). Grasslands on the  
318 other hand have shallow roots that are more susceptible to surface soil moisture variations (Yang et al., 2014).

319  
320 Not only the mean of the growing season temperature, but also its variability is crucial for explaining the significance of SSM  
321 and TWS for vegetation functioning **(Figure 4d)**. A higher temporal variability in temperature increases the importance of  
322 TWS for vegetation. This is because atmospheric water demand scales with temperature. Hence, higher variability in  
323 temperature implies more peaks in related atmospheric water demand which is a stronger incentive for plants to access deeper  
324 water storages which are more often available to meet the vegetation's transpiration demand.

325  
326 **Figure S8** illustrates the effect of the other six important predictors on the model output. Apart from climatological parameters  
327 (mean P, variability in  $R_n$ , and P, and aridity index), elevation and slope explain part of the variability in the relevance of SSM  
328 vs. TWS for NIRv. Although the reasons for increasing relevance of TWS for vegetation functioning at higher elevation remain  
329 unclear, it may be due to elevation's strong correlation with other climatic variables such as  $T_a$  and P.

### 330 **3.4 Robustness Tests**

331 Although NIRv can largely reflect vegetation functioning (Badgley et al., 2017), we repeat our analysis with SIF, which is an  
332 alternative and independent indicator for vegetation functioning and shows a near-linear relationship with gross primary



333 productivity at the ecosystem level (Guanter et al., 2012). However, SIF is only available at a coarse resolution of 0.5 degree.  
334 The partial correlations,  $r(\text{SIF} \sim \text{SSM})$  and  $r(\text{SIF} \sim \text{TWS})$  largely agree with the pattern of  $r(\text{NIRv} \sim \text{SSM})$  and  $r(\text{NIRv} \sim \text{TWS})$   
335 across varying aridity index and tree cover classes (**Figure S9**). This suggests that our overall conclusion on the relevance of  
336 SSM or TWS for vegetation functioning is robust across different indicators of vegetation productivity.

337

338 The partial correlation of NIRv with TWS is confounded by the presence of SSM within TWS, which makes it challenging to  
339 determine the relative importance of SSM and TWS for vegetation functioning. To address this issue, we re-calculated the  
340 partial correlation of NIRv with TWS while additionally controlling for SSM (next to  $T_a$  and  $R_n$ ) during growing season  
341 months. With this additional control variable, we observed fewer grid cells with positive and significant correlations compared  
342 to the analysis without controlling for SSM. Additionally, the magnitude of the partial correlation of NIRv with TWS slightly  
343 decreased in most grid cells when controlling for SSM (**Figure S10**). Nevertheless, we still observed the decreasing relevance  
344 of SSM and increasing relevance of TWS along an increasing tree cover fraction. Similar gradient across the aridity index is  
345 also observed in this analysis controlling for SSM. Thus, we conclude that our findings hold even after controlling for the  
346 effect of SSM in TWS.

#### 347 **4. Summary and Conclusions**

348 In this study we compare the relevance of near-surface soil moisture and of terrestrial water storage for vegetation functioning  
349 across the globe. We find that in semi-arid regions and regions with low tree cover, vegetation preferentially utilises the water  
350 from shallow soil, which is related to continuous availability of near-surface water availability and lack of deep rooting systems  
351 respectively. By contrast, in mostly forested regions and in relatively dry climate regimes, the correlation with terrestrial water  
352 storage is comparable or higher than with near-surface soil moisture, indicating that trees and vegetation in arid regions use  
353 their deep root systems to access deeper soil moisture.

354

355 We also find that vegetation's preferential water uptake depth changes over time. During particularly dry months, the relative  
356 importance of terrestrial water storage is higher, highlighting the importance of deep water resources during periods of low  
357 soil water availability. This is in line with previous studies showing changes in vegetation's water uptake depth during drought  
358 periods at small spatial scales where accessing water in deeper soil layers helps plants to alleviate water stress and maintain  
359 transpiration (Migliavacca et al., 2009; Tao et al., 2021).

360

361 Furthermore, we show that the spatial variability of the importance of near-surface soil moisture vs. terrestrial water storage  
362 for vegetation functioning is influenced by temperature and the fraction of tree cover. This emphasises the role of climate in  
363 determining shallow vs. deep soil water resources, and the role of vegetation in adapting to different soil water availability  
364 patterns.



365 Vegetation functioning and soil water storages are generally coupled in both directions, i.e. while soil moisture availability  
366 affects vegetation functioning (positive coupling), this in turn also affects soil moisture through transpiration (negative  
367 coupling). As our study focuses on water-controlled vegetation we only consider positive couplings and filter out grid cells  
368 with negative correlations. Future research may consider the relevance of soil moisture across depths for the positive coupling  
369 regions.

370  
371 Overall, our analysis illustrates that satellite-based data can be used for belowground analysis at large spatial scales thanks to  
372 the fact that satellite retrievals can assess soil water storage dynamics across depths and because vegetation in water-controlled  
373 areas can be used as an indicator of soil water dynamics. Such novel ways to improve our understanding of belowground water  
374 dynamics is necessary and valuable as respective in-situ observations are scarce and of limited representativeness for larger  
375 areas, particularly given the typical spatial heterogeneity of soils and vegetation. Our results can further inform a better  
376 representation of belowground processes in global models in order to support more accurate projections of future changes in  
377 climate, water resources, and ecosystem services.

#### 378 **Data availability**

379 The monthly SIF data is available from [https://www.gfz-potsdam.de/sektion/fernerkundungund-  
380 geoinformatik/projekte/global-monitoring-of-vegetation-fluorescence-globfluo/daten](https://www.gfz-potsdam.de/sektion/fernerkundungund-geoinformatik/projekte/global-monitoring-of-vegetation-fluorescence-globfluo/daten). The NIRv was calculated from the red  
381 and near-infrared reflectance obtained from the MOD13C1 v006 product (<https://lpdaac.usgs.gov/products/mod13c1v061/>).  
382 The ESA-CCI soil moisture can be accessed through <https://esa-soilmoisture-cci.org/> and Terrestrial Water Storage Anomaly  
383 data can be accessed through [https://podaac.jpl.nasa.gov/dataset/TELLUS\\_GRACGRFO\\_MASCON\\_CRI\\_GRID\\_RL06\\_V2](https://podaac.jpl.nasa.gov/dataset/TELLUS_GRACGRFO_MASCON_CRI_GRID_RL06_V2).  
384 The ERA5 climate variables are available from <https://www.ecmwf.int/en/forecasts/datasets/reanalysis-datasets/era5> . Tree  
385 cover fraction data is available from the AVHRR vegetation continuous fields products  
386 <https://lpdaac.usgs.gov/products/vcf5kyrv001/>, land cover data is available from <https://www.esa-landcover-cci.org/>, and  
387 topographic data is available via <https://www.earthenv.org/topography> . Similarly, the irrigation fraction data could be accessed  
388 from <https://mygeohub.org/publications/8> .

#### 389 **Competing Interests**

390 The contact author has declared that none of the authors has any competing interests.



391 **Acknowledgements**

392 The authors thank Ulrich Weber for help with obtaining and processing the data, and the Hydrology–Biosphere–Climate  
393 Interactions group at the Max Planck Institute for Biogeochemistry for fruitful discussions. Prajwal Khanal, Anne Hoek van  
394 Dijke and Rene Orth acknowledge funding by the German Research Foundation (Emmy Noether grant no. 391059971).

395 **References**

- 396 Amatulli, G., Domisch, S., Tuanmu, M.-N., Parmentier, B., Ranipeta, A., Malczyk, J., & Jetz, W. (2018). A suite of global,  
397 cross-scale topographic variables for environmental and biodiversity modeling. *Scientific Data*, 5(1), 180040.  
398 <https://doi.org/10.1038/sdata.2018.40>
- 399 Andrew Feldman, Gianotti, D., Dong, J., Akbar, R., Crow, W., McColl, K., Nippert, J., Tumber-Dávila, S. J., Holbrook, N.  
400 M., & al., F. R. et. (2022). Satellites capture soil moisture dynamics deeper than a few centimeters and are relevant  
401 to plant water uptake. *Earth and Space Science Open Archive*. <https://doi.org/10.1002/essoar.10511280.1> DA - 2022
- 402 Badgley, G., Field, C. B., & Berry, J. A. (2017). Canopy near-infrared reflectance and terrestrial photosynthesis. *Science*  
403 *Advances*, 3(3), e1602244. <https://doi.org/10.1126/sciadv.1602244>
- 404 Breiman, L. (2001). [No title found]. *Machine Learning*, 45(1), 5–32. <https://doi.org/10.1023/A:1010933404324>
- 405 Budyko, M. I. (1974). *Climate and life*. Academic press.
- 406 Capehart, W. J., & Carlson, T. N. (1997). Decoupling of surface and near-surface soil water content: A remote sensing  
407 perspective. *Water Resources Research*, 33(6), 1383–1395. <https://doi.org/10.1029/97WR00617>
- 408 Chen, T., & Guestrin, C. (2016). XGBoost: A Scalable Tree Boosting System. *Proceedings of the 22nd ACM SIGKDD*  
409 *International Conference on Knowledge Discovery and Data Mining*, 785–794.  
410 <https://doi.org/10.1145/2939672.2939785>
- 411 Denissen, J. M. C., Teuling, A. J., Pitman, A. J., Koirala, S., Migliavacca, M., Li, W., Reichstein, M., Winkler, A. J., Zhan,  
412 C., & Orth, R. (2022). Widespread shift from ecosystem energy to water limitation with climate change. *Nature*  
413 *Climate Change*, 12(7), 677–684. <https://doi.org/10.1038/s41558-022-01403-8>
- 414 Dorigo, W., Wagner, W., Albergel, C., Albrecht, F., Balsamo, G., Brocca, L., Chung, D., Ertl, M., Forkel, M., Gruber, A.,  
415 Haas, E., Hamer, P. D., Hirschi, M., Ikonen, J., de Jeu, R., Kidd, R., Lahoz, W., Liu, Y. Y., Miralles, D., ... Lecomte,





- 416 P. (2017). ESA CCI Soil Moisture for improved Earth system understanding: State-of-the art and future directions.  
417 *Remote Sensing of Environment*, 203, 185–215.
- 418 Fan, Y., Miguez-Macho, G., Jobbágy, E. G., Jackson, R. B., & Otero-Casal, C. (2017). Hydrologic regulation of plant rooting  
419 depth. *Proceedings of the National Academy of Sciences of the United States of America*, 114(40), 10572–10577.  
420 <https://doi.org/10.1073/pnas.1712381114>
- 421 Guanter, L., Frankenberg, C., Dudhia, A., Lewis, P. E., Gómez-Dans, J., Kuze, A., Suto, H., & Grainger, R. G. (2012).  
422 Retrieval and global assessment of terrestrial chlorophyll fluorescence from GOSAT space measurements. *Remote*  
423 *Sensing of Environment*, 121, 236–251. <https://doi.org/10.1016/j.rse.2012.02.006>
- 424 Hansen, Matthew, & Song, Xiao-Peng. (2018). *Vegetation Continuous Fields (VCF) Yearly Global 0.05 Deg* [Data set].  
425 NASA EOSDIS Land Processes DAAC. <https://doi.org/10.5067/MEASURES/VCF/VCF5KYR.001>
- 426 Hersbach, H., Bell, B., Berrisford, P., Hirahara, S., Horányi, A., Muñoz-Sabater, J., Nicolas, J., Peubey, C., Radu, R., Schepers,  
427 D., Simmons, A., Soci, C., Abdalla, S., Abellan, X., Balsamo, G., Bechtold, P., Biavati, G., Bidlot, J., Bonavita, M.,  
428 ... Thépaut, J.-N. (2020). The ERA5 global reanalysis. *Quarterly Journal of the Royal Meteorological Society*,  
429 146(730), 1999–2049. <https://doi.org/10.1002/qj.3803>
- 430 Humphrey, V., Zscheischler, J., Ciais, P., Gudmundsson, L., Sitch, S., & Seneviratne, S. I. (2018). Sensitivity of atmospheric  
431 CO<sub>2</sub> growth rate to observed changes in terrestrial water storage. *Nature*, 560(7720), 628–631.  
432 <https://doi.org/10.1038/s41586-018-0424-4>
- 433 Keenan, T. F., & Williams, C. A. (2018). The Terrestrial Carbon Sink. *Annual Review of Environment and Resources*, 43(1),  
434 219–243. <https://doi.org/10.1146/annurev-environ-102017-030204>
- 435 Köhler, P., Guanter, L., & Joiner, J. (2015). A linear method for the retrieval of sun-induced chlorophyll fluorescence from  
436 GOME-2 and SCIAMACHY data. *Atmos. Meas. Tech.*, 8(6), 2589–2608. <https://doi.org/10.5194/amt-8-2589-2015>
- 437 Koster, R. D., Guo, Z., Yang, R., Dirmeyer, P. A., Mitchell, K., & Puma, M. J. (2009). On the nature of soil moisture in land  
438 surface models. *Journal of Climate*, 22(16), 4322–4335. <https://doi.org/10.1175/2009JCLI2832.1>
- 439 Landerer, F. W., & Swenson, S. C. (2012). Accuracy of scaled GRACE terrestrial water storage estimates. *Water Resources*  
440 *Research*, 48(4). <https://doi.org/10.1029/2011WR011453>



- 441 Li, W., Migliavacca, M., Forkel, M., Denissen, J. M. C., Reichstein, M., Yang, H., Duveiller, G., Weber, U., & Orth, R. (2022).  
442 Widespread increasing vegetation sensitivity to soil moisture. *Nature Communications*, *13*(1), 3959.  
443 <https://doi.org/10.1038/s41467-022-31667-9>
- 444 Li, W., Migliavacca, M., Forkel, M., Walther, S., Reichstein, M., & Orth, R. (2021). Revisiting Global Vegetation Controls  
445 Using Multi-Layer Soil Moisture. *Geophysical Research Letters*, *48*(11). <https://doi.org/10.1029/2021GL092856>
- 446 Lundberg, S. M., Erion, G., Chen, H., DeGrave, A., Prutkin, J. M., Nair, B., Katz, R., Himmelfarb, J., Bansal, N., & Lee, S.-  
447 I. (2020). From local explanations to global understanding with explainable AI for trees. *Nature Machine Intelligence*,  
448 *2*(1), 56–67. <https://doi.org/10.1038/s42256-019-0138-9>
- 449 Migliavacca, M., Meroni, M., Manca, G., Matteucci, G., Montagnani, L., Grassi, G., Zenone, T., Teobaldelli, M., Goded, I.,  
450 Colombo, R., & Seufert, G. (2009). Seasonal and interannual patterns of carbon and water fluxes of a poplar plantation  
451 under peculiar eco-climatic conditions. *Agricultural and Forest Meteorology*, *149*(9), 1460–1476.  
452 <https://doi.org/10.1016/j.agrformet.2009.04.003>
- 453 Miguez-Macho, G., & Fan, Y. (2021). Spatiotemporal origin of soil water taken up by vegetation. *Nature*, *598*(7882), 624–  
454 628. <https://doi.org/10.1038/s41586-021-03958-6>
- 455 Mohammed, G. H., Colombo, R., Middleton, E. M., Rascher, U., van der Tol, C., Nedbal, L., Goulas, Y., Pérez-Priego, O.,  
456 Damm, A., Meroni, M., Joiner, J., Cogliati, S., Verhoef, W., Malenovský, Z., Gastellu-Etchegorry, J.-P., Miller, J.  
457 R., Guanter, L., Moreno, J., Moya, I., ... Zarco-Tejada, P. J. (2019). Remote sensing of solar-induced chlorophyll  
458 fluorescence (SIF) in vegetation: 50 years of progress. *Remote Sensing of Environment*, *231*, 111177.
- 459 Ohta, T., Kotani, A., Iijima, Y., Maximov, T. C., Ito, S., Hanamura, M., Kononov, A. V., & Maximov, A. P. (2014). Effects  
460 of waterlogging on water and carbon dioxide fluxes and environmental variables in a Siberian larch forest, 1998–  
461 2011. *Agricultural and Forest Meteorology*, *188*, 64–75. <https://doi.org/10.1016/j.agrformet.2013.12.012>
- 462 Orth, R. (2021). When the Land Surface Shifts Gears. *AGU Advances*, *2*(2). <https://doi.org/10.1029/2021AV000414>
- 463 Qiu, R., Li, X., Han, G., Xiao, J., Ma, X., & Gong, W. (2022). Monitoring drought impacts on crop productivity of the U.S.  
464 Midwest with solar-induced fluorescence: GOSIF outperforms GOME-2 SIF and MODIS NDVI, EVI, and NIRv.  
465 *Agricultural and Forest Meteorology*, *323*, 109038. <https://doi.org/10.1016/j.agrformet.2022.109038>



- 466 Reynolds, C. A., Jackson, T. J., & Rawls, W. J. (2000). Estimating soil water-holding capacities by linking the Food and  
467 Agriculture Organization Soil map of the world with global pedon databases and continuous pedotransfer functions.  
468 *Water Resources Research*, 36(12), 3653–3662. <https://doi.org/10.1029/2000WR900130>
- 469 Schenk, H. J., & Jackson, R. B. (2002). Rooting depths, lateral root spreads and below-ground/above-ground allometries of  
470 plants in water-limited ecosystems. *Journal of Ecology*, 90(3), 480–494. [https://doi.org/10.1046/j.1365-](https://doi.org/10.1046/j.1365-2745.2002.00682.x)  
471 [2745.2002.00682.x](https://doi.org/10.1046/j.1365-2745.2002.00682.x)
- 472 Seneviratne, S. I., Corti, T., Davin, E. L., Hirschi, M., Jaeger, E. B., Lehner, I., Orlowsky, B., & Teuling, A. J. (2010).  
473 *Investigating soil moisture-climate interactions in a changing climate: A review* (Vol. 99, Issues 3–4, pp. 125–161).  
474 <https://doi.org/10.1016/j.earscirev.2010.02.004>
- 475 Siebert, S., Kummu, M., Porkka, M., Döll, P., Ramankutty, N., & Scanlon, B. (2015). *Historical Irrigation Dataset (HID)*  
476 [Data set]. MyGeoHUB. <https://doi.org/10.13019/M20599>
- 477 Stocker, B. D., Tumber-Dávila, S. J., Konings, A. G., Anderson, M. C., Hain, C., & Jackson, R. B. (2023). Global patterns of  
478 water storage in the rooting zones of vegetation. *Nature Geoscience*, 16(3), 250–256. [https://doi.org/10.1038/s41561-](https://doi.org/10.1038/s41561-023-01125-2)  
479 [023-01125-2](https://doi.org/10.1038/s41561-023-01125-2)
- 480 Tao, Z., Neil, E., & Si, B. (2021). Determining deep root water uptake patterns with tree age in the Chinese loess area.  
481 *Agricultural Water Management*, 249, 106810.
- 482 Teuling, A. J., Hirschi, M., Ohmura, A., Wild, M., Reichstein, M., Ciais, P., Buchmann, N., Ammann, C., Montagnani, L.,  
483 Richardson, A. D., Wohlfahrt, G., & Seneviratne, S. I. (2009). A regional perspective on trends in continental  
484 evaporation. *Geophysical Research Letters*, 36(2). <https://doi.org/10.1029/2008GL036584>
- 485 Xie, X., He, B., Guo, L., Miao, C., & Zhang, Y. (2019). Detecting hotspots of interactions between vegetation greenness and  
486 terrestrial water storage using satellite observations. *Remote Sensing of Environment*, 231, 111259.
- 487 Yang, Y., Long, D., Guan, H., Scanlon, B. R., Simmons, C. T., Jiang, L., & Xu, X. (2014). GRACE satellite observed  
488 hydrological controls on interannual and seasonal variability in surface greenness over mainland Australia. *Journal*  
489 *of Geophysical Research: Biogeosciences*, 119(12), 2245–2260. <https://doi.org/10.1002/2014JG002670>

490  
491